

1 **Genetic mapping of sex and self-incompatibility determinants in the androdioecious**  
2 **plant *Phillyrea angustifolia***

3

4 **Authors:**

5 Amélie Carré<sup>1</sup>, Sophie Gallina<sup>1</sup>, Sylvain Santoni<sup>2</sup>, Philippe Vernet<sup>1</sup>, Cécile Godé<sup>1</sup>, Vincent Castric<sup>1</sup>, Pierre  
6 Saumitou-Laprade<sup>1#</sup>

7

8 **Affiliations :**

9 <sup>1</sup> CNRS, Univ. Lille, UMR 8198 – Evo-Eco-Paleo, F-59000 Lille, France

10 <sup>2</sup> UMR DIAPC - Diversité et adaptation des plantes cultivées

11

12

13 # **Corresponding author:** Pierre.Saumitou-Laprade@univ-lille.fr

14

15

16

17 **Abstract**

18 The diversity of mating and sexual systems in Angiosperms is spectacular, but the factors driving their  
19 evolution remain poorly understood. In plants of the Oleaceae family, an unusual self-incompatibility (SI)  
20 system has been discovered recently, whereby only two distinct homomorphic SI specificities segregate  
21 stably. To understand the role of this peculiar SI system in preventing or promoting the diversity of sexual  
22 phenotypes observed across the family, an essential first step is to characterize the genetic architecture  
23 of these two traits. Here, we developed a high-density genetic map of the androdioecious shrub *P.*  
24 *angustifolia* based on a F1 cross between a hermaphrodite and a male parent with distinct SI genotypes.  
25 Using a double restriction-site associated digestion (ddRAD) sequencing approach, we obtained reliable  
26 genotypes for 196 offspring and their two parents at 10,388 markers. The resulting map comprises 23  
27 linkage groups totaling 1,855.13 cM on the sex-averaged map. We found strong signals of association for  
28 the sex and SI phenotypes, that were each associated with a unique set of markers on linkage group 12  
29 and 18 respectively, demonstrating inheritance of these traits as single, independent, mendelian factors.  
30 The *P. angustifolia* linkage map shows robust synteny to the olive tree genome overall. Two of the six  
31 markers strictly associated with SI in *P. angustifolia* have strong similarity with a recently identified 741kb  
32 chromosomal region fully linked to the SI phenotype on chromosome 18 of the olive tree genome,  
33 providing strong cross-validation support. The SI locus stands out as being markedly rearranged, while the  
34 sex locus has remained relatively [more](#) collinear between the two species. This *P. angustifolia* linkage map  
35 will be a useful resource to investigate the various ways by which the sex and SI determination systems  
36 have co-evolved in the broader phylogenetic context of the Oleaceae family.

Supprimé: more

## 38 Introduction

39 Sexual reproduction is strikingly diverse across Angiosperms, both in terms of the proportion of  
40 autogamous vs. allogamous matings and in terms of the distribution of male and female sexual functions  
41 within and among individuals (BARRETT 1998; SAKAI AND WELLER 1999; DIGGLE *et al.* 2011). The conditions  
42 under which this diversity could arise under apparently similar ecological conditions and have evolved  
43 rapidly -sometimes even within the same family- have been a topic of intense interest in evolutionary  
44 biology (BARRETT 1998). The control of self-fertilization and the delicate balance between its costs and  
45 benefits is considered to be a central force driving this diversity. Avoidance of self-fertilization is  
46 sometimes associated with observable phenotypic variations among reciprocally compatible partners.  
47 These variations can be morphological (e.g. distyly) or temporal (e.g. protandry, protogyny in the case of  
48 heterodichogamy), but in many cases the flowers show no obvious morphological or phenological  
49 variation, and self-fertilization avoidance relies on so-called "homomorphic" self-incompatibility (SI)  
50 systems. These systems are defined as the inability of fertile hermaphrodite plants to produce zygotes  
51 through self-fertilization (LUNDQVIST 1956; DE NETTANCOURT 1977), and typically rely on the segregation of  
52 a finite number of recognition "specificities" whereby matings between individuals expressing cognate  
53 specificities are not successful at producing zygotes. At the genetic level, the SI specificities most  
54 commonly segregate as a single multi-allelic mendelian locus, the S locus. This locus contains at least two  
55 genes, one encoding the male determinant expressed in pollen and the other encoding the female  
56 determinant expressed in pistils, with the male specificity sometimes determined by a series of tandemly  
57 arranged paralogs (KUBO *et al.* 2015). The male and female determinants are both highly polymorphic and  
58 tightly linked, being inherited as a single non-recombining genetic unit. In cases where the molecular  
59 mechanisms controlling SI could be studied in detail, they were found to be remarkably diverse, illustrating  
60 their independent evolutionary origins across the flowering plants (IWANO AND TAKAYAMA 2012). Beyond  
61 the diversity of the molecular functions employed, SI systems **can** also differ in their genetic architecture.

Mis en forme : Non Première page différente

Supprimé: can

63 In the Poaceae family for example, two independent loci (named S and Z) control SI (Yang, et al., 2008). In  
64 other cases, the alternate allelic specificities can be determined by presence-absence variants rather than  
65 nucleotide sequence variants of a given gene, such as *e.g.* in *Primula vulgaris*, where one of the two  
66 reproductive phenotypes is hemizygous rather than heterozygous for the SI locus (LI *et al.* 2016).

Supprimé:

67 In spite of this diversity of molecular mechanisms and genetic architectures, a common feature of  
68 SI phenotypes is that they are all expected to evolve under negative frequency-dependent selection, a  
69 form of natural selection favoring the long-term maintenance of high levels of allelic diversity (WRIGHT  
70 1939). Accordingly, large numbers of distinct SI alleles are commonly observed to segregate within natural  
71 and cultivated SI species (reviewed in CASTRIC AND VEKEMANS 2004). There are notable exceptions to this  
72 general rule, however, and in some species only two SI specificities seem to segregate stably. Most often  
73 in such diallelic SI systems, the two SI specificities are in perfect association with morphologically  
74 distinguishable floral phenotypes. In distylous species, for instance, two floral morphs called “pin” (L-  
75 morph) and “thrum” (S-morph) coexist (BARRETT 1992; BARRETT 2019). In each morph, the anthers and  
76 stigma are spatially separated within the flowers, but located at corresponding, reciprocal positions  
77 between the two morphs. Additional morphological differences exist, with S-morph flowers producing  
78 fewer but larger pollen grains than L-morph flowers (DULBERGER 1992). These morphological differences  
79 are believed to enhance the selfing avoidance conferred by the SI system but also to increase both male  
80 and female fitnesses (BARRETT 1990; BARRETT 2002; KELLER *et al.* 2014), although it is not clear which of SI  
81 or floral morphs became established in the first place (CHARLESWORTH AND CHARLESWORTH 1979).

82 The Oleacea family is another intriguing exception, where a diallelic SI system was recently found  
83 to be shared across the entire family (VERNET *et al.* 2016). In this family of trees, the genera *Jasminum* ( $2n$   
84 = 26), *Fontanesia* ( $2n = 26$ ) and *Forsythia* ( $2n = 28$ ) are all heterostylous and are therefore all expected to  
85 possess a heteromorphic diallelic SI system; in *Jasminum fruticans* self- and within-morph fertilization are  
86 unsuccessful (DOMMÉE *et al.* 1992). The ancestral heterostyly gave rise to species with hermaphrodite (e.g.

Supprimé: self-incompatibility

Supprimé: ancestral

Supprimé:  $2x =$

Supprimé:  $2x =$

Supprimé:  $= 2x$

Supprimé: seem

Supprimé: self-incompatibility

95 *Ligustrum vulgare*, *Olea europaea*), androdioecious (e.g. *P. angustifolia*, *Fraxinus ornus*), polygamous (e.g.  
96 *Fraxinus excelsior*) and even dioecious (e.g. *Fraxinus chinensis*) sexual systems, possibly in association with  
97 a doubling of the number of chromosomes ( $2n= 46$  in the Oleaceae tribe). Evaluation of pollen germination  
98 success by controlled *in vitro* crossing experiments (stigma test) revealed the existence of a previously  
99 unsuspected homomorphic diallelic SI, in one of these species, *P. angustifolia* (SAUMITOU-LAPRADE *et al.*  
100 2010). In this androdioecious species (i.e. in which male and hermaphrodite individuals coexist in the same  
101 populations), hermaphrodite individuals form two morphologically indistinguishable groups of SI  
102 specificities that are reciprocally compatible but incompatible within groups, whereas males show  
103 compatibility with hermaphrodites of both groups (SAUMITOU-LAPRADE *et al.* 2010). This “universal”  
104 compatibility of males offsets the reproductive disadvantage they suffer from lack of their female function,  
105 such that the existence of the diallelic SI system provides a powerful explanation to the long-standing  
106 evolutionary puzzle represented by the maintenance of high frequencies of males in this species (PANNELL  
107 AND KORBECKA 2010; SAUMITOU-LAPRADE *et al.* 2010; BILLIARD *et al.* 2015; PANNELL AND VOILLEMOT 2015).  
108 Extension of the stigma test developed in *P. angustifolia* to other species of the same tribe including *L.*  
109 *vulgaris* (DE CAUWER *et al.* 2020), *F. ornus* (VERNET *et al.* 2016) and *O. europaea* (SAUMITOU-LAPRADE *et al.*  
110 2017; DUPIN *et al.* 2020) demonstrated that all species exhibited some form of the diallelic SI system, but  
111 with no consistent association with floral morphology. Cross-species pollination experiments even showed  
112 that pollen from *P. angustifolia* is able to trigger a robust SI response on *O. europaea* and the more distant  
113 *F. ornus* and *F. excelsior* stigmas (the reciprocal is also true). This opens the question of whether the  
114 homomorphic diallelic SI determinants are orthologs across the Oleaceae tribe, even in the face of the variety  
115 of sexual polymorphisms present in the different species. More broadly, its link with the heteromorphic  
116 diallelic SI determinant in the ancestral diploid, largely heterostylous, species remains to be established  
117 (BARRETT 2019). Understanding the causes of the long-term maintenance of this SI system and exploring  
118 its consequences on the evolution of sexual systems in hermaphrodite, androdioecious, polygamous or

Mis en forme : Retrait : Première ligne : 0 cm

Supprimé: *F. excelsior*) and even dioecious (e.g. *F. chinensis*) sexual systems, possibly in association with a doubling of the number of chromosomes ( $2n = 2x = 46$  in the Oleaceae tribe). Detailed crossing experiments in one of these species, *P. angustifolia*, revealed the existence of a previously unsuspected homomorphic diallelic self-incompatibility.

Supprimé: self-incompatibility

Supprimé: more distant

Supprimé: self-incompatibility

Supprimé: self-incompatibility determinant is identical (orthologous)

Supprimé: self-incompatibility

132 dioecious species of the family represents an important goal. The case of *P. angustifolia* is particularly  
133 interesting because it is one of the rare instances where separate sexes decoupled from mating types can  
134 be studied in a single species (CHARLESWORTH 1978).

**Supprimé:** *angustifolia* is particularly interesting because it is one of the rare instances where separate sexes and the diallelic self-incompatibility system can be studied in a single species, and therefore lies at the crossroads of processes that may be obscured in lineages where they are unfolding independently (ROSAS AND DOMÍNGUEZ 2009; BARRETT 2010; LIU *et al.* 2012; BILLIARD *et al.* 2015)

135 A first step toward a better understanding of the role of the diallelic SI system in promoting the  
136 sexual diversity in Oleaceae is to characterize and compare the genetic architecture of the SI and sexual  
137 phenotypes. At this stage, however, the genomic resources for most of these non-model species remain  
138 limited. In this context, the recent sequencing efforts (UNVER *et al.* 2017; JIMÉNEZ-RUIZ *et al.* 2020) and the  
139 genetic mapping of the SI locus in a biparental population segregating for SI groups in *Olea europaea*  
140 (MARIOTTI *et al.* 2020) represent major breakthroughs in the search for the SI locus in Oleaceae. They have  
141 narrowed down the SI locus to an interval of 5.4cM corresponding to a region of approximately 300kb, but  
142 it is currently unknown whether the same region is controlling SI in other species. In *P. angustifolia*, based  
143 on a series of genetic analysis of progenies from controlled crosses, Billiard *et al.* (2015) proposed a fairly  
144 simple genetic model, where sex and SI are controlled by two independently segregating diallelic loci.  
145 Under this model, sex would be determined by the “M” locus at which a dominant allele *M* codes for the  
146 male phenotype (*i.e.* *M* is a female-sterility mutation leading e.g. to arrested development of the stigma)  
147 and a recessive allele *m* codes for the hermaphrodite phenotype. The S locus would encode the SI system  
148 and comprise a dominant allele *S2* and a recessive allele *S1*. The model thus hypothesizes that  
149 hermaphrodites are homozygous *mm* at the sex locus, and fall into two groups of SI specificities, named  
150 *H<sub>a</sub>* and *H<sub>b</sub>* carrying the *S1S1* and *S1S2* genotypes at the S locus, respectively (their complete genotypes  
151 would thus be *mmS1S1* and *mmS1S2* respectively). The model also hypothesizes three male genotypes  
152 (*M<sub>a</sub>*: *mMS1S1*, *M<sub>b</sub>*: *mMS1S2*, and *M<sub>c</sub>*: *mMS2S2*). In addition, Billiard *et al.* (2015) showed that, while males  
153 are compatible with all hermaphrodites, the segregation of sexual phenotypes varies according to which  
154 group of hermaphrodites they sire: the progeny of *H<sub>a</sub>* hermaphrodites pollinated by males systematically  
155 consists of both hermaphrodites and males with a consistent but slight departure from 1:1 ratio, while

**Supprimé:** self-incompatibility

**Supprimé:** offspring

**Supprimé:** hermaphrodite

**Supprimé:** segregates

167 that of H<sub>b</sub> hermaphrodites pollinated by the very same males systematically consists of male individuals  
168 only. This observation suggests a pleiotropic effect of the *M* allele, conferring not only female sterility and  
169 universal pollen compatibility, but also a complete male-biased sex-ratio distortion when crossed with one  
170 of the two groups of hermaphrodites and a more subtle departure from 1:1 ratio when crossed with the  
171 other group of hermaphrodites (BILLIARD *et al.* 2015). The latter departure, however, was observed on  
172 small progeny arrays only, and its magnitude thus comes with considerable uncertainty.

173 In this study, we developed a high-density genetic map for the non-model tree *P. angustifolia* using  
174 a ddRAD sequencing approach and used it to address three main questions related to the evolution of its  
175 peculiar reproductive system. First, are the SI and sex phenotypes in *P. angustifolia* encoded by just two  
176 independent loci, as predicted by the most likely segregation model of Billiard *et al.* (2015)? Second, which  
177 specific genomic regions are associated with the SI and sex loci, and what segregation model do the SI and  
178 sex-associated loci follow (i.e. which of the males or hermaphrodites, and which of the two SI phenotypes  
179 are homozygous vs. heterozygous at either loci, or are these phenotypes under the control of hemizygous  
180 genomic regions?). Third, what is the level of synteny between our *P. angustifolia* genetic map and the  
181 recently published Olive tree genome (UNVER *et al.* 2017; MARIOTTI *et al.* 2020), both globally and  
182 specifically at the SI and sex-associated loci?

183

## 184 **Material and Methods**

### 185 **Experimental cross and cartography population**

186 In order to get both the SI group and the sexual phenotype (males vs hermaphrodites) to segregate  
187 in a single progeny array, a single maternal and a single paternal plant were chosen among the progenies  
188 of the controlled crosses produced by (BILLIARD *et al.* 2015). Briefly, a H<sub>a</sub> maternal tree (named 01.N-25,  
189 with putative genotype mmS1S1) was chosen in the progeny of a (H<sub>a</sub> x M<sub>a</sub>) cross. It was crossed in March  
190 2012 to a M<sub>b</sub> father (named 13.A-06, putative genotype mM S1S2) chosen in the progeny of a (H<sub>a</sub> x M<sub>c</sub>)  
191 cross, following the protocol of Saumitou-Laprade *et al.* (2010). Both trees were maintained at the

192 experimental garden of the “Plateforme des Terrains d'Expérience du LabEx CeMEB,” (CEFE, CNRS) in  
193 Montpellier, France. F1 seeds were collected in September 2012 and germinated in the greenhouse of the  
194 “Plateforme Serre, cultures et terrains expérimentaux,” at the University of Lille (France). Seedling  
195 paternity was verified with two highly polymorphic microsatellite markers (VASSILIADIS *et al.* 2002), and  
196 1,064 plants with confirmed paternity were installed in May 2013 on the experimental garden of the  
197 “Plateforme des Terrains d'Expérience du LabEx CeMEB,” (CEFE, CNRS) in Montpellier. Sexual phenotypes  
198 were visually determined based on the absence of stigma for 1,021 F1 individuals during their first  
199 flowering season in 2016 and 2017 (absence of stigma indicates male individuals). Twenty-one progenies  
200 did not flower and 22 died during the test period. The hermaphrodite individuals were assigned to an SI  
201 group using the stigma test previously described in Saumitou-Laprade *et al.* (2010; SAUMITOU-LAPRADE *et al.*  
202 2017).

Supprimé: Gender

Supprimé: Among

Supprimé: , 21

#### 204 DNA extraction, library preparation and sequencing

205 In 2015, *i.e.* the year before sexual phenotypes were determined and stigma tests were  
206 performed, 204 offspring were randomly selected for genomic library preparation and genotyping. Briefly,  
207 DNA from parents and progenies was extracted from 100 mg of frozen young leaves with the Chemagic  
208 DNA Plant Kit (Perkin Elmer Chemagen, Baesweiler, DE, Part # CMG-194), according to the manufacturer’s  
209 instructions. The protocol was adapted to the use of the KingFisher Flex™ (Thermo Fisher Scientific,  
210 Waltham, MA, USA) automated DNA purification workstation. The extracted DNA was quantified using a  
211 Qubit fluorometer (Thermo Fisher Scientific, Illkirch, France). Genome complexity was reduced by Double  
212 Digestion Restriction Associated DNA sequencing (ddRAD seq) (PETERSON *et al.* 2012) using two restriction  
213 enzymes: *Pst*I, a rare-cutting restriction enzyme sensitive to methylation recognizing the motif CTGCA/G,  
214 and *Mse*I, a common-cutting restriction enzyme recognizing the motif T/TAA. The libraries were  
215 constructed at the INRAE - AGAP facilities (Montpellier, France). Next-generation sequencing was

Supprimé: phenotyping

Supprimé: test

Supprimé: random

Supprimé: were

223 performed in a 150-bp paired-ends-read mode using three lanes on a HiSeq3000 sequencer (Illumina, San  
224 Diego, CA, USA) at the Get-Plage core facility (Genotoul platform, INRAE Toulouse, France).

## 225 GBS data analysis and linkage mapping

226 Illumina sequences were quality filtered with the *process\_radtags* program of Stacks v2.3  
227 (CATCHEN *et al.* 2011) to remove low quality base calls and adapter sequences. We followed the Rochette  
228 & Catchen protocol (ROCHETTE AND CATCHEN 2017) to obtain a *de novo* catalog of reference loci. Briefly, the  
229 reads were assembled and aligned with a minimum stack depth of 3 ( $-m=3$ ) and at most two nucleotide  
230 differences when merging stacks into loci ( $-M=2$ ). We allowed at most two nucleotide differences between  
231 loci when building the catalog ( $-n=2$ ). Both parental and all offspring FASTQ files were aligned to the *de*  
232 *novo* catalog using Bowtie2 v2.2.6 (LANGMEAD AND SALZBERG 2012), the option 'end-to-end' and 'sensitive'  
233 were used for the alignment. At this step, one .bam file was obtained per individual to construct the linkage  
234 map with Lep-MAP3\_ (RASTAS 2017). A custom python script was used to remove SPNs markers with reads  
235 coverage <5. After this step, the script *calls* Samtools v1.3.1 and the script *pileupParser2.awk* (limit1=5) to  
236 convert .bam files to the format used by Lep-MAP3. We used the *ParentCall2* module of Lep-MAP3 to  
237 select loci with reliable parental genotypes by considering genotype information on parents and offspring.  
238 The *Filtering2* module was then used to remove non-informative and distorted markers (dataTolerance =  
239 0.0000001). The module *SeparateChromosomes2* assigned markers to linkage groups (LGs), after test,  
240 where the logarithm of odds score (LodLimit) varied from 10 to 50 in steps of 5 then from 20 to 30 in steps  
241 of 1 and the minimum number of SNP markers (sizeLimit) per linkage group from 50 to 500 in steps of 50  
242 for each of the LodLimit. The two parameters, lodLimit = 27 and sizeLimit = 250, were chosen as the best  
243 parameters to obtain the 23 linkage groups (as expected in members of the Oleoideae subfamily;  
244 WALLANDER AND ALBERT 2000). A custom python script removed loci with SNPs markers mapped on two or  
245 more different linkage groups. The last module *OrderMarkers2* ordered the markers within each LG. To  
246 consider the slight stochastic variation in marker distances between executions, the module was run three

**Supprimé:** and then aligned to a *de novo* catalog created from parents and progeny of the cross. According to

**Supprimé:** some parameters are tested

**Supprimé:** assembly and alignment steps. The following Stacks parameters

**Supprimé:** used:

**Supprimé:** ), at most two nucleotide differences when merging stacks into loci ( $-M=2$ ),

**Supprimé:** cover

**Supprimé:** call

**Supprimé:** good

**Supprimé:** format

259 times on each linkage group, first separately for the meiosis that took place in each parent (sexAveraged  
260 = 0) and then averaged between the two parents (sexAveraged = 1). To produce the most likely final father  
261 and mother specific maps and a final sex-averaged maps (DE-KAYNE AND FEULNER 2018), we kept for each  
262 map the order of markers that had the highest likelihoods for each linkage group. In the end of some  
263 linkage groups, we removed from the final genetic map markers that were clearly outliers i.e. that had  
264 orders of magnitude more recombination to any marker than the typical average (Table 1). The original  
265 map is provided in Figure S1.

## 267 Sex and SI locus identification

268 To identify the sex-determination system in *P. angustifolia* we considered two possible genetic  
269 models. First, a “XY” male heterogametic system, where males are heterozygous or hemizygous (XY) and  
270 hermaphrodites are homozygous (XX). Second, a “ZW” hermaphrodite heterogametic system, where  
271 hermaphrodites are heterozygous or hemizygous (ZW) and males are homozygous (ZZ). We applied the  
272 same logic to the SI determination system, as segregation patterns (Billiard et al. 2015) suggested that SI  
273 possibly also has a heterogametic determination system, with homozygous H<sub>a</sub> and heterozygous H<sub>b</sub>. In the  
274 same way as for sex, it is therefore possible to test the different models (XY, ZW or hemizygous) to  
275 determine which SNPs are linked to the two SI phenotypes.

276 Based on this approach, we identified sex-linked and SI-linked markers on the genetic map by  
277 employing SEX-DETECTOR, a maximum-likelihood inference model initially designed to distinguish  
278 autosomal from sex-linked genes based on segregation patterns in a cross (MUYLE *et al.* 2016). Briefly, a  
279 new alignment of reads from each individual on the loci used to construct the linkage map was done with  
280 bwa (LI AND DURBIN 2009). This new alignment has the advantage of retrieving more SNPs than used by  
281 LepMap3, as SNPs considered as non-informative by LepMap3 can still be informative to distinguish among  
282 sex- or SI-determination systems by SEX-DETECTOR. The alignment was analyzed using Reads2snp (default

Supprimé: probabilistic model based on

Supprimé: .

285 tool for SEX-DETECTOR) (TSAGKOGEOGA *et al.* 2012), with option -par 0. We ran Reads2snp without the -aeb  
286 (account for allelic expression bias) option to accomodate for the use of genomic rather than RNA-seq  
287 data. For each phenotype (H<sub>a</sub> vs. H<sub>b</sub> and males vs. hermaphrodites), SEX-DETECTOR was run for both a XY  
288 and a ZW model with the following parameters: -detail, -L, -SEM, -thr 0.8, -E 0.05. For each run, SEX-  
289 DETECTOR also calculates the probability for X (or Z)-hemizygous segregation in the heterozygous  
290 haplotypes. To compensate for the heterogeneity between the number of males (83) and hermaphrodites  
291 (113) in our progeny array, each model was tested three times with sub-samples of 83 hermaphrodites  
292 obtained by randomly drawing from the 113 individuals. We retained SNPs with a ≥80% probability of  
293 following an XY (or ZW) segregation pattern, with a minimum of 50% of genotyped individuals and less  
294 than 5% of the individuals departing from this model (due to either genotyping error or crossing-over).

Supprimé: .

295

#### 296 **Synteny analysis with the olive tree**

297 To study synteny, we used Basic Local Alignment Search Tool (BLAST) to find regions of local  
298 similarity between the *P. angustifolia* ddRADseq loci in the linkage map and the *Olea europea var. sylvestris*  
299 genome assembly (UNVER *et al.* 2017). This assembly is composed of 23 main chromosomes and a series  
300 of 41,233 unanchored scaffolds for a total of 1,142,316,613 bp. Only loci with a unique hit with at least  
301 85% identity over a minimum of 110 bp were selected for synteny analysis. Synteny relationships were  
302 visualized with *circos-0.69-6* (KRZYWINSKI *et al.* 2009). Synteny between linkage groups of *P. angustifolia*  
303 and the main 23 *O. europea* chromosomes was established based on the number of markers with a  
304 significant BLAST hit. At a finer scale, we also examined synteny with the smaller unanchored scaffolds of  
305 the assembly, as the history of rearrangement and allo-tetraploidization is likely to have disrupted synteny.

Supprimé: the

308

309 **Data availability**

310 Fastq files for all 204 offspring and both parents are deposited in the NCBI BioProject (SRA  
311 accession PRJNA724813). All scripts used can be accessed at [https://github.com/Amelie-Carre/Genetic-  
map-of-Phillyrea-angustifolia](https://github.com/Amelie-Carre/Genetic-<br/>312 map-of-Phillyrea-angustifolia) .

313

Supprimé: ¶  
¶

316 **Results**

317 **Phenotyping progenies for sex and SI groups**

318 As expected, our cartography population segregated for sex and SI phenotypes, providing a  
319 powerful resource to genetically map these two traits. Among the 1,021 F1 individuals that flowered  
320 during the two seasons of phenotyping, we scored 619 hermaphrodites and 402 males, revealing a biased  
321 sex ratio in favor of hermaphrodites ( $khi^2= 1.28 \times 10^{-11}$ ). Stigma tests were successfully performed on 613  
322 hermaphrodites (6 individuals flowered too late to be included in a stigma test), revealing 316 H<sub>a</sub> and 297  
323 H<sub>b</sub>, i.e. an equilibrated segregation of the two SI phenotypes ( $khi^2= 0.27$ ). The random subsample of 204  
324 F1 progenies chosen before the first flowering season for ddRAD-seq analysis (see below) followed similar  
325 phenotypic proportions. 196 of the 204 progenies ended up flowering, revealing 83 males and 113  
326 hermaphrodites, among which 60 belonged to the H<sub>a</sub> group and 53 to the H<sub>b</sub> group.

327

328 **Linkage mapping**

329 The two parents and the 196 offspring that had flowered were successfully genotyped using a  
330 ddRAD-seq approach. Our stringent filtering procedure identified 11,070 loci composed of 17,096 SNP  
331 markers as being informative for Lep-MAP3. By choosing a LOD score of 27, 10,388 loci composed of  
332 15,814 SNPs were assigned to, and arranged within, 23 linkage groups in both sex-averaged and sex-  
333 specific maps (Table 1).

334 The linkage groups of the mother map were on average larger (78.88 cM) than the linkage groups  
335 of the father map (73.40 cM) and varied from 22.73 cM to 112.38 cM and from 35 cM to 121.94 cM  
336 respectively (Table 1, Figure S1). The total map lengths were 1586.57 cM, 1688.16 cM and 1814.19 cM in  
337 the sex-averaged, male and female maps, respectively. The length of the linkage groups varied from 23.90  
338 cM to 110.69 cM in the sex-averaged map, with an average of 683 SNPs markers per linkage group (Table  
339 1).

Supprimé: With the chosen

Supprimé: 84.45

Supprimé: 77.84

Supprimé: 54.14

Supprimé: 133.40

Supprimé: 56.06

Supprimé: 131.66

Supprimé: 1,855.13

Supprimé: 1,790.33

Supprimé: 1,942.30

Supprimé: 59.10

Supprimé: 129.70

Supprimé: 687

Supprimé:

354

355 **Sex and SI locus identification**

356 We found evidence that a region on linkage group 18 (LG18) is associated with the SI phenotypes,  
 357 with Hb hermaphrodites having heterozygous genotype, akin to a XY system. Indeed, when comparing H<sub>a</sub>  
 358 and H<sub>b</sub>, among the 38,998 SNPs analyzed by SEX-DETECTOR, 496 have a probability of following an XY  
 359 pattern  $\geq 0.80$ . We then applied two stringent filters by retaining only SNPs that had been genotyped for  
 360 more than 50% of the offspring (n=211), and for which less than 5% of the offspring departed from the  
 361 expected genotype under a XY model (n=23). Six of these 23 SNPs, distributed in 4 loci, followed a  
 362 segregation pattern strictly consistent with a XY model. These four loci are tightly clustered on the linkage  
 363 map and define a region of 1.230 cM on LG18 (Figure 1) in the sex-averaged map. Relaxing the stringency  
 364 or our thresholds, this region also contains five loci that strictly follow an XY segregation but with less than  
 365 50% of offsprings successfully genotyped, as well as six loci with autosomal inheritance, possibly  
 366 corresponding to polymorphisms accumulated within allelic lineages associated with either of the  
 367 alternate SI specificities. Using the same filtering scheme, none of the SNPs was found to follow a ZW  
 368 pattern.

Supprimé: When

Supprimé: ).

Supprimé: .

Supprimé: This provides evidence that this region on LG18 is associated with the SI phenotypes, with a determination system akin to a XY system where H<sub>b</sub> have the heterogametic genotype.¶

369 For the comparison of male and hermaphrodites, an average of 44,565 SNPs were analyzed by  
 370 SEX-DETECTOR across the three subsamples, among which an average of 438 have a probability of following  
 371 an XY pattern  $\geq 0.80$ . We applied the same set of stringent filters and retained an average of 171 SNPs  
 372 having been genotyped for at least 50% of the offspring, among which 41 have less than 5% of the offspring  
 373 departing from the expected genotype under a XY model and are shared across the three subsets. Thirty-  
 374 two of these SNPs followed a segregation pattern strictly consistent with a XY model. These 32 markers,  
 375 corresponding to 8 loci, are distributed along a region of 2.216 cM on linkage group 12 (LG12, Figure 1) in  
 376 the sex-averaged map. Relaxing the stringency or our thresholds, this region also contains five loci that  
 377 strictly follow an XY segregation pattern but with less than 50% of offspring successfully genotyped, as

Supprimé:

Supprimé: ).

387 well as 17 loci consistent with autosomal inheritance, possibly corresponding to polymorphisms  
388 accumulated within allelic lineages associated with either of the alternate sex specificities. Again, no SNP  
389 was found to follow a ZW pattern. This provides evidence that this independent region on LG12 is  
390 associated with sex, with a determination system akin to a XY system where males have the heterogametic  
391 genotype.

Supprimé: .

392

### 393 Synteny analysis with the olive tree

394 About half (49%) of the 10,388 *P. angustifolia* loci used for the genetic map had a significant BLAST  
395 hit on the olive tree genome. Overall, the relative position of these hits was highly concordant with the  
396 structure of the linkage map. Indeed, the vast majority (79.7%) of loci belonging to a given linkage group  
397 have non-ambiguous matches on the same olive tree chromosome. Loci that did not follow this general  
398 pattern did not cluster on other chromosomes, suggesting either small rearrangements or  
399 mapping/assembly errors at the scale of individual loci. The order of loci within the linkage groups was  
400 also well conserved with only limited evidence for rearrangements (Figure 2, Figure 3), suggesting that the  
401 two genomes have remained largely collinear.

Supprimé: find hits in particularly clustered regions

Supprimé: overall

402 We then specifically inspected synteny between the linkage groups carrying either the sex or the  
403 SI locus and the olive tree genome (Figure 4). Synteny was good for LG12, the linkage group containing the  
404 markers associated with the sex phenotype. Among the 645 loci of LG12, 365 have good homology in the  
405 olive tree genome. Eighty eight percent had their best hits on the same chromosome of the olive tree  
406 (chromosome 12 per our numbering of the linkage groups), and the order of markers was largely  
407 conserved along this chromosome. Six loci contained in the region associated with sex on LG12 had hits  
408 on a single 1,940,009bp region on chromosome 12. This chromosomal interval contains 82 annotated  
409 genes in the olive tree genome (Table S1). In addition, eight loci in the sex region had their best hits on a  
410 series of five smaller scaffolds (Sca393, Sca1196, Sca1264, Sca32932, Sca969) that could not be reliably

Supprimé: find

Supprimé: small

Supprimé: 81

Supprimé: .

418 anchored in the main olive tree assembly but may nevertheless also contain candidates for sex  
419 determination. Collectively, these scaffolds represent 1.849.345bp of sequence in the olive tree genome  
420 and contain 57 annotated genes ([Table S1](#)).

Supprimé: 47

Supprimé: .

421 Synteny was markedly poorer for markers on LG18, the linkage group containing the markers  
422 associated with the SI specificity phenotypes (Figure 5). Of the 440 loci on LG18, 203 have non-ambiguous  
423 BLAST hits on the olive tree genome. Although a large proportion (89%) had their best hits on chromosome  
424 18, the order of hits along that chromosome suggested a large number of rearrangements. This more  
425 rearranged order was also observed for the six markers that were strictly associated with SI in *P.*  
426 *angustifolia*. Two of them had hits on a single region of 741,403bp on the olive tree genome. This region  
427 contains 32 annotated genes ([Table S2](#)) and contains two markers that were previously found to be  
428 genetically associated with SI directly in the olive tree by Mariotti *et al.* (2020). Three markers more loosely  
429 associated with SI in *P. angustifolia* found hits on a more distant region on chromosome 18 (19,284,909-  
430 19,758,630Mb). The three other strongly associated markers all had hits on scaffold 269, which contains  
431 15 annotated genes and represents 545,128bp. Nine other loci strongly or loosely associated with SI had  
432 hits on a series of seven other unanchored scaffolds (Sca1199, Sca1200, Sca1287, Sca1579, Sca213,  
433 Sca327, Sca502) that collectively represent 96 annotated genes ([Table S2](#)) and 2,539,637bp.

Supprimé: 11

Supprimé: .

Supprimé: 78

Supprimé: .

Supprimé: .

## 435 Discussion

436 Until now, studies have mostly relied on theoretical or limited genetic segregation analyses to  
437 investigate the evolution of sexual and SI phenotypes in *P. angustifolia* (VASSILIADIS *et al.* 2002; SAUMITOU-  
438 LAPRADE *et al.* 2010; HUSSE *et al.* 2013; BILLIARD *et al.* 2015). In this study, we created the first genetic map  
439 of the androdioecious species *P. angustifolia* and identified the genomic regions associated with these two  
440 important reproductive phenotypes. The linkage map we obtained shows strong overall synteny with the

448 olive tree genome, and reveals that sex and SI phenotypes segregate independently from one another,  
449 and are each strongly associated with a different genomic region (in LG18 and LG12, respectively).

450 The SI linked markers on LG18 are orthologous with the genomic interval recently identified by  
451 Mariotti *et al.* (2020) as the region controlling SI in the domesticated olive tree, providing strong reciprocal  
452 support that the determinants of SI are indeed located in this region. Interestingly, we observed a series  
453 of shorter scaffolds that could not previously be anchored in the main assembly of the olive tree genome  
454 but match genetic markers that are strictly linked to SI in *P. angustifolia*. These unanchored scaffolds  
455 provide a more complete set of genomic sequences that will be important to consider in the perspective  
456 of identifying the (currently elusive) molecular determinants of SI in these two species. We note that poor  
457 assembly of the S-locus region (MARIOTTI *et al.* 2020) was expected given the considerable levels of  
458 structural rearrangements typically observed in SI- and more generally in the mating type-determining  
459 regions (GOUBET *et al.* 2012; BADOUIN *et al.* 2015), making *P. angustifolia* a useful resource to map the SI  
460 locus in the economically important species *O. europaea*.

461 Our observations also provide direct support to the hypothesis that the determinants of SI have  
462 remained at the same genomic position at least since the two lineages diverged, 30 to 40 Myrs ago  
463 (BESNARD *et al.* 2009; OLOFSSON *et al.* 2019). Stability of the genomic location of SI genes has been observed  
464 in some Brassicaceae species, where the *SRK-SCR* system maps at orthologous positions in the Arabidopsis  
465 and Capsella genera (GUO *et al.* 2011). In other Brassicaceae species, however, the SI system is found at  
466 different genomic locations, such as in Brassica and Leavenworthia. In the former, the molecular  
467 determinants have remained orthologous (also a series of *SRK-SCR* pairs, (IWANO *et al.* 2014), but not in  
468 the latter, where SI seems to have evolved *de novo* from exaptation of a pair of paralogous genes (CHANTHA  
469 *et al.* 2013; CHANTHA *et al.* 2017). Together with the fact that *P. angustifolia* pollen is able to trigger a robust  
470 SI response on *O. europaea* stigmas (SAUMITOU-LAPRADE *et al.* 2017), our results provide strong support to  
471 the hypothesis that the *P. angustifolia* and *O. europaea* SI systems are orthologous.

Supprimé: syntenic

Supprimé: in the

Supprimé: are syntenic to

Supprimé: was indeed

Supprimé: more distant

Supprimé: the synteny we observed provides

478 Several approaches could now be used to refine the mapping location in *P. angustifolia*, and  
479 ultimately zero in on the molecular determinants of SI. One possibility would require fine-mapping using  
480 larger offspring arrays, starting from our cross for which only a fraction of all phenotyped individuals were  
481 genotyped. Beyond the analysis of this controlled cross, evaluating whether the association of the SI  
482 phenotype still holds for markers within a larger set of accessions from diverse natural populations will  
483 constitute a powerful fine-mapping approach. Since the SI phenotypes seem to be functionally  
484 orthologous across the Oleaceae tribe (VERNET *et al.* 2016), the approach could, in principle, be extended to  
485 more distant SI species of the family like *L. vulgare* or *F. ornus*. Identification of sequences that have  
486 remained linked over these considerable time scales would represent excellent corroborative evidence to  
487 validate putative SI candidates. In parallel, an RNA-sequencing approach could be used to identify  
488 transcripts specific to the alternate SI phenotypes.

Supprimé: A first

Supprimé: whose association holds

489 While comparison to the closely related *O. europaea* genome is a useful approach for the mapping  
490 of SI in *P. angustifolia*, it is *a priori* of limited use for mapping the sex-determining region, since the olive  
491 tree lineage has been entirely hermaphroditic for at least 32.22 Myrs (confidence interval: 28-36 Myrs)  
492 (FigS1 in OLOFSSON *et al.* 2019). Detailed exploration of the genomic region in the olive tree that is  
493 orthologous to the markers associated with sex in *P. angustifolia* is however interesting, as it may either  
494 have anciently played a role in sex determination and subsequently lost it, or alternatively it may contain  
495 quiescent sex-determining genes that have been activated specifically in *P. angustifolia*. At a broader scale,  
496 mapping and eventually characterizing the sex locus in other androdioecious species such as e.g. *F. ornus*  
497 could indicate whether the different instances of androdioecy in the family represent either orthologous  
498 phenotypes or independent evolutionary emergences.

Supprimé:

Supprimé: happen to

Supprimé: along the

Supprimé: specifically

499 Identifying the molecular mechanisms of the genes controlling SI and sex and tracing their  
500 evolution in a phylogenetic context would prove extremely useful. First, it could help understand the  
501 strong functional pleiotropy between sex and SI phenotypes, whereby males express universal SI

508 compatibility (SAUMITOU-LAPRADE *et al.* 2010). In other words, males are able to transmit the SI specificities  
509 they inherited from their parents, but they do not express them themselves even though their pollen is  
510 fully functional. This intriguing feature of the SI system was key to solve the puzzle of why *P. angustifolia*  
511 maintains unusually high frequencies of males in natural populations (HUSSE *et al.* 2013), but the question  
512 of how being a male prevents expression of the SI phenotype in pollen is still open. A possibility is that the  
513 *M* allele of the sex locus contains a gene interacting negatively either with the pollen SI determinant itself  
514 or with a gene of the downstream response cascade. Identifying the molecular basis of this epistasis will  
515 be an interesting next step. Second, another intriguing feature of the system is segregation distortion, that  
516 is observed at several levels. Billiard *et al.* (2015) observed complete segregation bias in favor of male  
517 offspring of  $H_b$  hermaphrodites sired by males. Here, by phenotyping >1,000 offspring of a  $H_a$   
518 hermaphrodite sired by a  $M_b$  male, we confirmed that this cross also entails a departure from Mendelian  
519 segregation, this time in favor of hermaphrodites, albeit of a lesser magnitude. Although the generality of  
520 this observation still remains to be determined by careful examination of the other possible crosses ( $H_a$   
521 hermaphrodites x  $M_a$  and  $M_c$  males), it is clear that segregation distortion is a general feature of this  
522 system, as was already observed in other sex determination systems causing departures from equal sex  
523 ratios (e.g. KOZIELSKA *et al.* 2010). Beyond the identification of the mechanisms by which the distortions  
524 arise, pinpointing the evolutionary conditions leading to their emergence will be key to understanding the  
525 role they may have played in the evolution of this reproductive system.

526 More broadly, while sex and mating types are confounded in many species across the tree of life  
527 and cannot be distinguished, the question of when and how sex and mating types evolve separately raises  
528 several questions. The evolution of anisogamy (and hence, sexual differentiation) has been linked to that  
529 of mating types (CHARLESWORTH 1978). In volvocine algae for instance, the mating-type locus in isogamous  
530 species is orthologous to the pair of U/V sex chromosomes in anisogamous/oogamous species, suggesting  
531 that the sex-determination system derives from the mating-type determination system (GENG *et al.* 2014).

Supprimé: an

Supprimé: question

Supprimé: fully aligned

535 From this perspective the Oleaceae family is an interesting model system, where a SI system is ancestral,  
536 and in which some species have evolved sexual specialization that is aligned with the two SI phenotypes  
537 (e.g. in the polygamous *F. excelsior* males belong to the H<sub>a</sub> SI group and can only mate with hermaphrodites  
538 or females of the H<sub>b</sub> group, and the sexual system of *F. excelsior* can be viewed as subdioecy (SAUMITOU-  
539 LAPRADE *et al.* 2018). In other species, sexual phenotypes are disjoint from SI specificities and led to the  
540 differentiation of males and hermaphrodites. For instance, in the androdieocious *P. angustifolia* and  
541 probably *F. ornus*, the male determinant is genetically independent from the SI locus but fully linked to a  
542 genetic determinant causing the epistatic effect over SI (BILLIARD *et al.* 2015; VERNET *et al.* 2016). Yet other  
543 species have remained perfect hermaphrodites and have no trace of sexual differentiation whatsoever (*O.*  
544 *europaeae*). Understanding why some species have followed one evolutionary trajectory while others have  
545 followed another will be an exciting avenue for future research (BILLIARD *et al.* 2011).

Supprimé: specialization is

Supprimé: (e.g.

Supprimé: perfectly

Supprimé: .

## 547 Author Contributions

548 All authors contributed to the study presented in this paper. PS-L and PV developed, designed and oversaw  
549 the study; they coordinated the cross and carried out the phenotyping and stigma tests. CG performed the  
550 seedling paternity analysis. SS performed DNA extraction, library preparation and organized sequencing.  
551 AC and SG constructed the data analysis pipeline and AC, SS, PS-L and VC interpreted the results and wrote  
552 the manuscript.

## 554 Acknowledgements

555 We thank Sylvain Bertrand and Fantin Carpentier for technical help for the phenotyping and Jos Käfer for  
556 scientific discussion and help in applying Sex-DETECTOR to our material. We thank Jacques Lepart†,  
557 Mathilde Dufay, Pierre Olivier Cheptou, Xavier Vekemans, Sylvain Billiard and Bénédicte Felter for scientific  
558 discussions. Field and laboratory work for phenotyping were done at the Platform Terrains d'Expériences

563 (Labex CeMEB ANR-10-LABX-0004-CeMEB) of the Centre d'Ecologie Fonctionnelle et Evolutive (CEFE,  
564 CNRS) with the help of Thierry Mathieu and David Degueldre and at the platform Serres cultures et terrains  
565 expérimentaux of the Lille University with the help of Nathalie Faure and Angélique Bourceaux. We are  
566 grateful to Marie-Pierre Dubois for providing access to the microscopy facilities at the SMGE (Service des  
567 Marqueurs Génétiques en Ecologie) platform (CEFE). This work was funded by the French National  
568 Research Agency through the project 'TRANS' (ANR-11-BSV7- 013-03) and by a grant from the European  
569 Research Council (NOVEL project, grant #648321). A.C was supported by a doctoral grant from the French  
570 ministry of research. The authors also thank the Région Hauts-de-France, and the Ministère de  
571 l'Enseignement Supérieur et de la Recherche (CPER Climibio), and the European Fund for Regional  
572 Economic Development for their financial support. We also thank the HPC Computing Mésocentre of the  
573 University of Lille which provided us with the computing grid. [We thank Tatiana Giraud and two](#)  
574 [anonymous referees for constructive reviews of an earlier version.](#)  
575

576 **References**

- 577 Badouin, H., M. E. Hood, J. Gouzy, G. Aguilera, S. Siguenza *et al.*, 2015 Chaos of  
578 Rearrangements in the Mating-Type Chromosomes of the Anther-Smut Fungus  
579 *Microbotryum lychnidis-dioicae*. *Genetics* 200: 1275-1284.
- 580 Barrett, S. C., 2002 The evolution of plant sexual diversity. *Nature Reviews Genetics* 3: 274-284.
- 581 Barrett, S. C. H., 1990 The evolution and adaptive significance of heterostyly. *Trends in Ecology*  
582 & Evolution 5: 144-148.
- 583 Barrett, S. C. H., 1992 Heterostylous Genetic Polymorphisms: Model Systems for Evolutionary  
584 Analysis, pp. 1-29 in *Evolution and Function of Heterostyly*, edited by S. C. H. Barrett.  
585 Springer Berlin Heidelberg, Berlin, Heidelberg.
- 586 Barrett, S. C. H., 1998 The evolution of mating strategies in flowering plants. *Trends in Plant*  
587 Science 3: 335-341.
- 588 Barrett, S. C. H., 2019 'A most complex marriage arrangement': recent advances on heterostyly  
589 and unresolved questions. *New Phytologist* 224: 1051-1067.
- 590 Besnard, G., R. Rubio de Casas, P.-A. Christin and P. Vargas, 2009 Phylogenetics of *Olea*  
591 (Oleaceae) based on plastid and nuclear ribosomal DNA sequences: Tertiary climatic  
592 shifts and lineage differentiation times. *Annals of Botany* 104: 143-160.
- 593 Billiard, S., L. Husse, P. Lapercq, C. Gode, A. Bourceaux *et al.*, 2015 Selfish male-determining  
594 element favors the transition from hermaphroditism to androdioecy. *Evolution* 69: 683-  
595 693.
- 596 Billiard, S., M. López-Villavicencio, B. Devier, M. E. Hood, C. Fairhead *et al.*, 2011 Having sex,  
597 yes, but with whom? Inferences from fungi on the evolution of anisogamy and mating  
598 types. *Biological Reviews* 86: 421-442.
- 599 Castric, V., and X. Vekemans, 2004 Plant self-incompatibility in natural populations: a critical  
600 assessment of recent theoretical and empirical advances. *Molecular Ecology* 13: 2873-  
601 2889.
- 602 Catchen, J. M., A. Amores, P. Hohenlohe, W. Cresko and J. H. Postlethwait, 2011 Stacks:  
603 building and genotyping Loci de novo from short-read sequences. *G3 (Bethesda, Md.)* 1:  
604 171-182.
- 605 Chantha, S.-C., A. C. Herman, V. Castric, X. Vekemans, W. Marande *et al.*, 2017 The unusual S  
606 locus of *Leavenworthia* is composed of two sets of paralogous loci. *New Phytologist* 216:  
607 1247-1255.
- 608 Chantha, S.-C., A. C. Herman, A. E. Platts, X. Vekemans and D. J. Schoen, 2013 Secondary  
609 Evolution of a Self-Incompatibility Locus in the Brassicaceae Genus *Leavenworthia*.  
610 *PLOS Biology* 11: e1001560.
- 611 Charlesworth, B., 1978 The population genetics of anisogamy. *Journal of Theoretical Biology*  
612 73: 347-357.
- 613 Charlesworth, D., and B. Charlesworth, 1979 A Model for the Evolution of Distyly. *The American*  
614 Naturalist 114: 467-498.
- 615 De-Kayne, R., and P. G. D. Feulner, 2018 A European Whitefish Linkage Map and Its  
616 Implications for Understanding Genome-Wide Synteny Between Salmonids Following  
617 Whole Genome Duplication. *G3 (Bethesda)* 8: 3745-3755.
- 618 De Cauwer, I., P. Vernet, S. Billiard, C. Godé, A. Bourceaux *et al.*, 2020 Widespread  
619 coexistence of self-compatible and self-incompatible phenotypes in a diallelic self-  
620 incompatibility system in *Ligustrum vulgare* (Oleaceae). *bioRxiv*:  
621 2020.2003.2026.009399.
- 622 De Nettancourt, D., 1977 *Incompatibility in Angiosperms*. Springer-Verlag, Berlin, Heidelberg et  
623 New York.

624 Diggle, P. K., V. S. Di Stilio, A. R. Gschwend, E. M. Golenberg, R. C. Moore *et al.*, 2011 Multiple  
625 developmental processes underlie sex differentiation in angiosperms. *Trends in Genetics*  
626 27: 368-376.

627 Dommée, B., J. D. Thompson and F. Cristini, 1992 Distylie chez *Jasminum fruticans* L.:  
628 hypothèse de la pollinisation optimale basée sur les variations de l'écologie intraflorale.  
629 *Bulletin de la Société Botanique de France. Lettres Botaniques* 139: 223-234.

630 Dulberger, R., 1992 Floral Polymorphisms and Their Functional Significance in the  
631 Heterostylous Syndrome, pp. 41-84 in *Evolution and Function of Heterostyly*, edited by S.  
632 C. H. Barrett. Springer Berlin Heidelberg, Berlin, Heidelberg.

633 Dupin, J., P. Raimondeau, C. Hong-Wa, S. Manzi, M. Gaudeul *et al.*, 2020 Resolving the  
634 Phylogeny of the Olive Family (Oleaceae): Confronting Information from Organellar and  
635 Nuclear Genomes. *Genes* 11: 1508.

636 Geng, S., P. De Hoff and J. G. Umen, 2014 Evolution of sexes from an ancestral mating-type  
637 specification pathway. *PLoS biology* 12: e1001904-e1001904.

638 Goubet, P. M., H. Bergès, A. Bellec, E. Prat, N. Helmstetter *et al.*, 2012 Contrasted Patterns of  
639 Molecular Evolution in Dominant and Recessive Self-Incompatibility Haplotypes in  
640 *Arabidopsis*. *PLOS Genetics* 8: e1002495.

641 Guo, Y.-L., X. Zhao, C. Lanz and D. Weigel, 2011 Evolution of the S-locus region in *Arabidopsis*  
642 relatives. *Plant physiology* 157: 937-946.

643 Husse, L., S. Billiard, J. Lepart, P. Vernet and P. Saumitou-Laprade, 2013 A one-locus model of  
644 androdioecy with two homomorphic self-incompatibility groups: expected vs. observed  
645 male frequencies. *Journal of evolutionary biology* 26: 1269-1280.

646 Iwano, M., K. Ito, H. Shimosato-Asano, K.-S. Lai and S. Takayama, 2014 Self-Incompatibility in  
647 the Brassicaceae, pp. 245-254 in *Sexual Reproduction in Animals and Plants*, edited by  
648 H. Sawada, N. Inoue and M. Iwano. Springer Japan, Tokyo.

649 Iwano, M., and S. Takayama, 2012 Self/non-self discrimination in angiosperm self-incompatibility.  
650 *Current Opinion in Plant Biology* 15: 78-83.

651 Jiménez-Ruiz, J., J. A. Ramírez-Tejero, N. Fernández-Pozo, M. d. I. O. Leyva-Pérez, H. Yan *et*  
652 *al.*, 2020 Transposon activation is a major driver in the genome evolution of cultivated  
653 olive trees (*Olea europaea* L.). *The Plant Genome* 13: e20010.

654 Keller, B., J. D. Thomson and E. Conti, 2014 Heterostyly promotes disassortative pollination and  
655 reduces sexual interference in Darwin's primroses: evidence from experimental studies.  
656 *Functional Ecology* 28: 1413-1425.

657 Kozielska, M., F. J. Weissing, L. W. Beukeboom and I. Pen, 2010 Segregation distortion and the  
658 evolution of sex-determining mechanisms. *Heredity* 104: 100-112.

659 Krzywinski, M. I., J. E. Schein, I. Birol, J. Connors, R. Gascoyne *et al.*, 2009 Circos: An  
660 information aesthetic for comparative genomics. *Genome Research*.

661 Kubo, K.-i., T. Paape, M. Hatakeyama, T. Entani, A. Takara *et al.*, 2015 Gene duplication and  
662 genetic exchange drive the evolution of S-RNase-based self-incompatibility in *Petunia*.  
663 *Nature Plants* 1: 1-9.

664 Langmead, B., and S. L. Salzberg, 2012 Fast gapped-read alignment with Bowtie 2. *Nature*  
665 *methods* 9: 357-359.

666 Li, H., and R. Durbin, 2009 Fast and accurate short read alignment with Burrows-Wheeler  
667 transform. *Bioinformatics* 25: 1754-1760.

668 Li, J., J. M. Cocker, J. Wright, M. A. Webster, M. McMullan *et al.*, 2016 Genetic architecture and  
669 evolution of the S locus supergene in *Primula vulgaris*. *Nature plants* 2: 16188.

670 Lundqvist, A., 1956 Self-incompatibility in rye. *Hereditas* 42: 293-348.

671 Mariotti, R., S. Pandolfi, I. De Cauwer, P. Saumitou-Laprade, P. Vernet *et al.*, 2020 Diallelic self-  
672 incompatibility is the main determinant of fertilization patterns in olive orchards.  
673 *Evolutionary Applications* n/a.

674 Muyle, A., J. Kafer, N. Zemp, S. Mousset, F. Picard *et al.*, 2016 SEX-DETECTOR: A Probabilistic  
675 Approach to Study Sex Chromosomes in Non-Model Organisms. *Genome Biol Evol* 8:  
676 2530-2543.

677 Olofsson, J. K., I. Cantera, C. Van de Paer, C. Hong-Wa, L. Zedane *et al.*, 2019 Phylogenomics  
678 using low-depth whole genome sequencing: A case study with the olive tribe. *Molecular*  
679 *Ecology Resources* 19: 877-892.

680 Pannell, J. R., and G. Korbecka, 2010 Mating-System Evolution: Rise of the Irresistible Males.  
681 *Current Biology* 20: R482-R484.

682 Pannell, J. R., and M. Voillemot, 2015 Plant mating systems: female sterility in the driver's seat.  
683 *Current Biology* 25: R511-514.

684 Peterson, B. K., J. N. Weber, E. H. Kay, H. S. Fisher and H. E. Hoekstra, 2012 Double digest  
685 RADseq: an inexpensive method for de novo SNP discovery and genotyping in model  
686 and non-model species. *PLoS One* 7: e37135.

687 Rastas, P., 2017 Lep-MAP3: robust linkage mapping even for low-coverage whole genome  
688 sequencing data. *Bioinformatics* 33: 3726-3732.

689 Rochette, N. C., and J. M. Catchen, 2017 Deriving genotypes from RAD-seq short-read data  
690 using Stacks. *Nature Protocols* 12: 2640-2659.

691 Sakai, A. K., and S. G. Weller, 1999 Gender and Sexual Dimorphism in Flowering Plants: A  
692 review of Terminology, Biogeographic Patterns, Ecological Correlates, and Phylogenetic  
693 Approaches, pp. 1-31 in *Gender and Sexual Dimorphism in Flowering Plants*, edited by  
694 M. A. Geber, T. E. Dawson and L. F. Delph. Springer Berlin Heidelberg, Berlin,  
695 Heidelberg.

696 Saumitou-Laprade, P., P. Vernet, A. Dowkiw, S. Bertrand, S. Billiard *et al.*, 2018 Polygamy or  
697 subdioecy? The impact of diallelic self-incompatibility on the sexual system in *Fraxinus*  
698 *excelsior* (Oleaceae). *Proceedings. Biological sciences* 285: 20180004.

699 Saumitou-Laprade, P., P. Vernet, C. Vassiliadis, Y. Hoareau, G. de Magny *et al.*, 2010 A self-  
700 incompatibility system explains high male frequencies in an androdioecious plant.  
701 *Science* 327: 1648-1650.

702 Saumitou-Laprade, P., P. Vernet, X. Vekemans, S. Billiard, S. Gallina *et al.*, 2017 Elucidation of  
703 the genetic architecture of self-incompatibility in olive: Evolutionary consequences and  
704 perspectives for orchard management. *Evolutionary Applications*: 1-14.

705 Tsagkogeorga, G., V. Cahais and N. Galtier, 2012 The population genomics of a fast evolver:  
706 high levels of diversity, functional constraint, and molecular adaptation in the tunicate  
707 *Ciona intestinalis*. *Genome Biol Evol* 4: 740-749.

708 Unver, T., Z. Wu, L. Sterck, M. Turktas, R. Lohaus *et al.*, 2017 Genome of wild olive and the  
709 evolution of oil biosynthesis. *Proceedings of the National Academy of Sciences of the*  
710 *United States of America* 114: E9413-e9422.

711 Vassiliadis, C., P. Saumitou-Laprade, J. Lepart and F. Viard, 2002 High male reproductive  
712 success of hermaphrodites in the androdioecious *Phillyrea angustifolia*. *Evolution* 56:  
713 1362-1373.

714 Vernet, P., P. Lepercq, S. Billiard, A. Bourceaux, J. Lepart *et al.*, 2016 Evidence for the long-  
715 term maintenance of a rare self-incompatibility system in Oleaceae. *New Phytologist*  
716 210: 1408-1417.

717 Wallander, E., and V. A. Albert, 2000 Phylogeny and classification of Oleaceae based on rps16  
718 and trnL-F sequence data. *American Journal of Botany* 87: 1827-1841.

719 Wright, S., 1939 The Distribution of Self-Sterility Alleles in Populations. *Genetics* 24: 538-552.

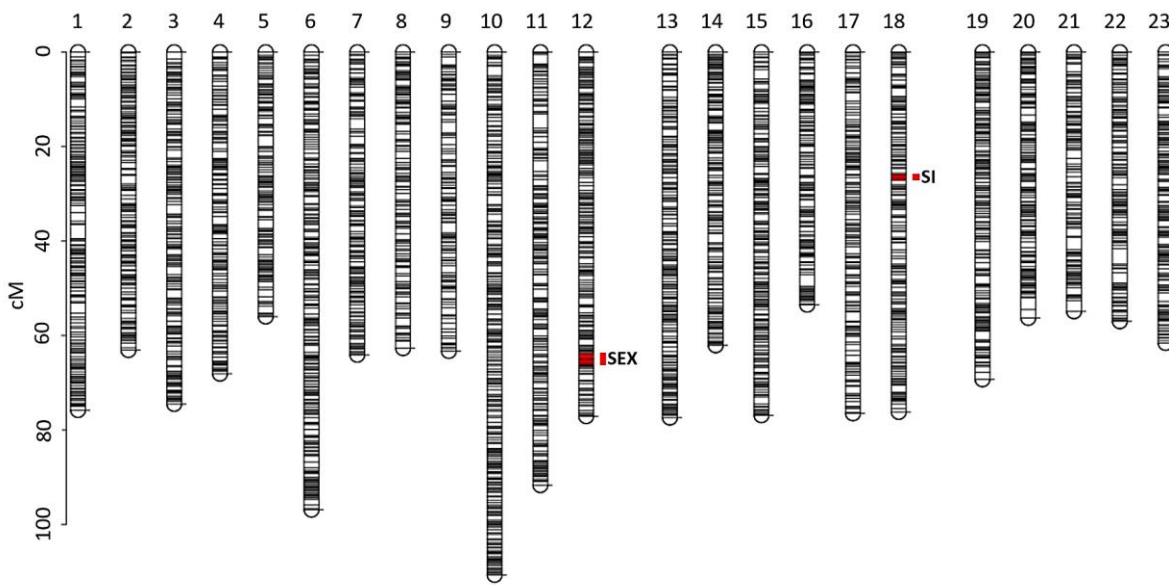
720

721

722 **Table 1.** Comparison of the sex-averaged, male and female linkage maps. The values in this table  
723 are computed without the outliers SNPs markers at the extremity of the linkage groups.  
724

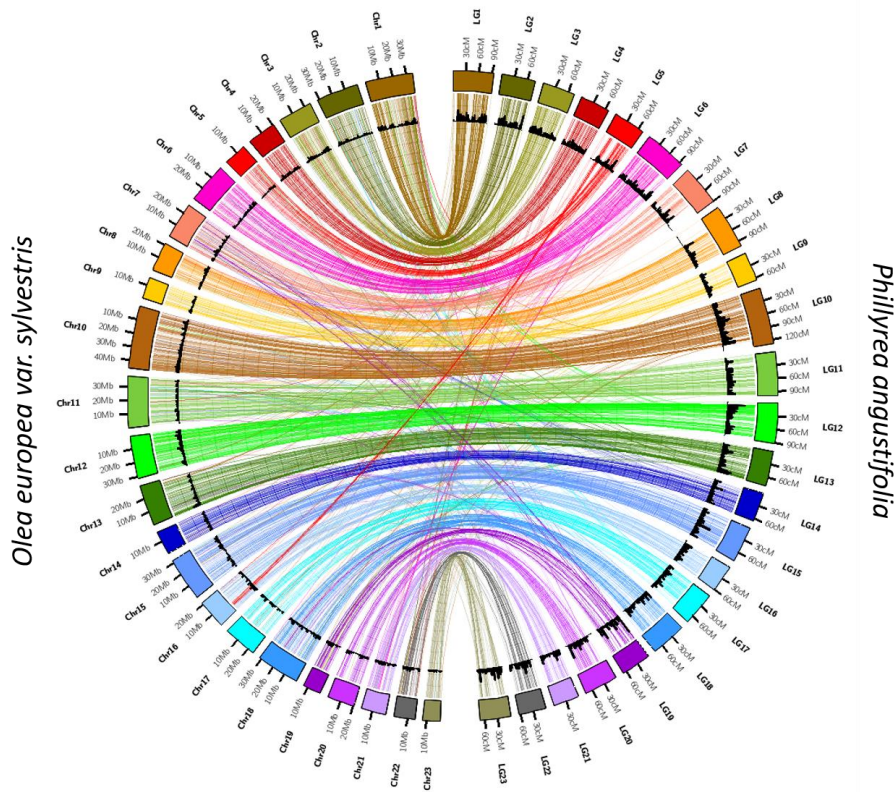
Linkage group	Number of SNPs	Number of SNPs (without outliers)	Sex-averaged map			Paternal map			Maternal map		
			LG length (cM)	SNPs/cM	average intermarker distance	LG Length (cM)	SNPs/cM	average intermarker distance	LG Length (cM)	SNPs/cM	average intermarker distance
1	854	839	75.78	11.07	0.09	79.30	10.58	0.09	92.11	9.11	0.11
2	633	621	23.90	25.98	0.10	35.00	17.74	0.12	22.73	27.32	0.11
3	676	676	74.50	9.07	0.11	61.94	10.91	0.09	85.42	7.91	0.13
4	535	535	68.07	7.86	0.13	71.63	7.47	0.13	69.82	7.66	0.13
5	502	494	56.02	8.82	0.11	50.58	9.77	0.10	67.84	7.28	0.14
6	877	877	96.89	9.05	0.11	90.81	9.66	0.10	103.63	8.46	0.12
7	609	601	64.14	9.37	0.11	68.93	8.72	0.11	64.99	9.25	0.11
8	486	479	62.71	7.64	0.13	91.89	5.21	0.19	119.25	4.02	0.25
9	408	406	63.28	6.42	0.16	56.06	7.24	0.14	71.04	5.72	0.18
10	1365	1361	110.69	12.30	0.08	121.95	11.16	0.09	112.38	12.11	0.08
11	793	783	91.66	8.54	0.12	80.40	9.74	0.10	108.84	7.19	0.14
12	973	969	77.12	12.56	0.08	91.52	10.59	0.09	88.09	11.00	0.09
13	849	848	77.40	10.96	0.09	77.29	10.97	0.09	80.77	10.50	0.10
14	566	565	62.12	9.10	0.11	72.25	7.82	0.13	71.39	7.91	0.13
15	750	747	76.92	9.71	0.10	82.98	9.00	0.11	96.01	7.78	0.13
16	591	589	53.53	11.00	0.09	56.93	10.35	0.10	69.56	8.47	0.12
17	613	613	76.52	8.01	0.13	70.58	8.69	0.12	83.94	7.30	0.14
18	660	659	76.22	8.65	0.12	77.26	8.53	0.12	81.99	8.04	0.12
19	806	806	69.29	11.63	0.09	91.10	8.85	0.11	79.49	10.14	0.10
20	547	531	56.26	9.44	0.11	67.56	7.86	0.13	62.91	8.44	0.12
21	479	476	54.86	8.68	0.12	69.49	6.85	0.15	54.14	8.79	0.11
22	550	544	57.05	9.54	0.11	55.64	9.78	0.10	61.44	8.85	0.11
23	690	684	61.64	11.10	0.09	67.10	10.19	0.10	66.42	10.30	0.10
<b>average</b>	<b>687</b>	<b>682</b>	<b>68.98</b>	<b>10.28</b>	<b>0.11</b>	<b>73.40</b>	<b>9.46</b>	<b>0.11</b>	<b>78.88</b>	<b>9.29</b>	<b>0.12</b>

725 **Figure 1.** *Phillyrea angustifolia* sex-averaged linkage map showing the grouping and position of 10,388  
726 SNPs. The length of each of the 23 linkage groups is indicated by the vertical scale in cM. The markers  
727 strictly linked to sex and self-incompatibility (SI) phenotypes are shown in red. Markers that were clearly  
728 outliers at the end of some linkage groups were removed (see Table1, Figure S1).

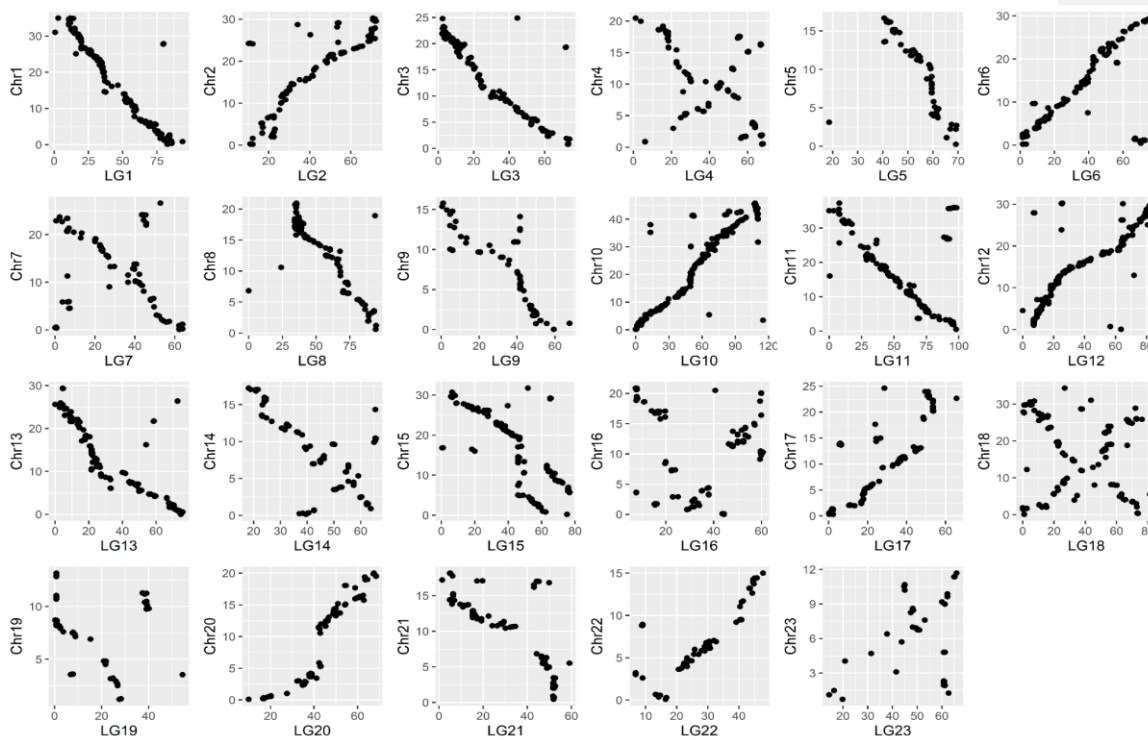


729 **Figure 2.** Synteny plot identifying homologous *P. angustifolia* linkage groups (LG, scale in cM) with olive  
 730 tree chromosomes (Chr, scale in Mb). Lines connect markers in the *P. angustifolia* linkage map with their  
 731 best BLAST hit in the *O. europea* genome and are colored according to the linkage group. Variation of the  
 732 density of loci in bins of 3.125cM along linkage groups and 1 Mbp along chromosomes is shown in the  
 733 inner circle as a black histogram.

Supprimé: (coloring according to their LG color)

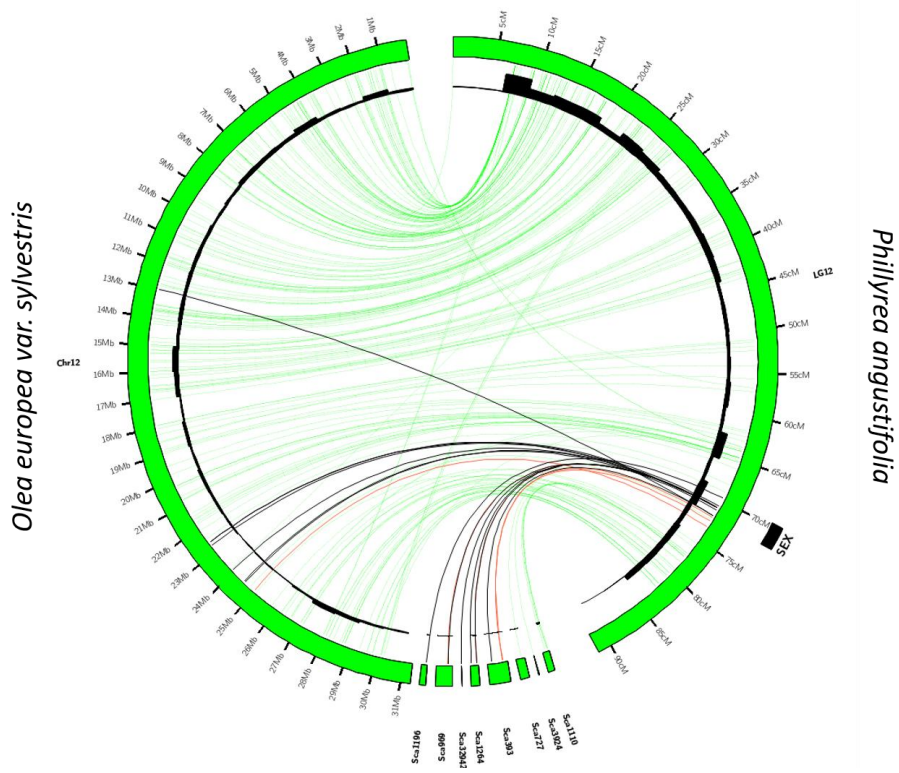


736 **Figure 3.** Visualization of chromosome-scale synteny by comparing the location of markers along the *P.*  
 737 *angustifolia* linkage groups (LG, scale in cM) with the location of their best BLAST hit along the homologous  
 738 olive tree chromosome (Chr, scale in Mbp). The vertical lines on LG12 and LG18 indicate the position of  
 739 markers strictly associated with sex and SI phenotypes in *P. angustifolia*, respectively. The horizontal line  
 740 on Chr18 indicates the chromosomal region containing the SI locus in *Olea europaea* according to Mariotti  
 741 *et al.* (2020).  
 742



743 **Figure 4.** Synteny plot between the *P. angustifolia* linkage group 12 (scale in cM) and the olive tree  
 744 chromosomes 12 and a series of unanchored scaffolds (scale in Mb). Lines connect markers in the *P.*  
 745 *angustifolia* linkage map with their best BLAST hit in the *O. europea* genome. Green lines correspond to  
 746 markers with autosomal inheritance. Black lines correspond to markers which strictly cosegregate with sex  
 747 phenotypes (males vs. hermaphrodites). Red lines correspond to markers with strong but partial (95%)  
 748 association with sex. Variation of the density of loci in bins of 3.125cM along linkage groups and 1 Mbp  
 749 along chromosomes is shown in the inner circle as a black histogram.

750



751 **Figure 5.** Synteny plot between the *P. angustifolia* linkage group 18 (scale in cM) and the olive tree  
 752 chromosomes 18 and a series of unanchored scaffolds (scale in Mb). Lines connect markers in the *P.*  
 753 *angustifolia* linkage map with their best BLAST hit in the *O. europea* genome. Blue lines correspond to  
 754 markers with autosomal inheritance. Black lines correspond to markers which strictly cosegregate with SI  
 755 phenotypes (H<sub>a</sub> vs. H<sub>b</sub>). Red lines correspond to markers with strong but partial (95%) association with SI.  
 756 The region found to be genetically associated with SI in the olive tree by Mariotti *et al.* (2020) is shown by  
 757 a black rectangle. Variation of the density of loci in bins of 3.125cM along linkage groups and 1 Mbp along  
 758 chromosomes is shown in the inner circle as a black histogram.

